Cell, Vol. 111, 471–481, November 15, 2002, Copyright ©2002 by Cell Press

A Thiol Peroxidase Is an H_2O_2 Receptor and Redox-Transducer in Gene Activation

Agnès Delaunay,[1] Delphine Pflieger,[2] Marie-Bénédicte Barrault,[1] Joelle Vinh,[2] and Michel B. Toledano[1,3]

[1]Laboratoire Stress Oxydants et Cancers
SBGM
DBJC
CEA-Saclay
91191 Gif-sur-Yvette
Cedex
France

[2]Laboratoire de Neurobiologie et Diversité Cellulaire
CNRS
UMR 7637
ESPCI
10, rue Vauquelin
75231 Paris
Cedex 05
France

Summary

The Yap1 transcription factor regulates hydroperoxide homeostasis in *S. cerevisiae*. Yap1 is activated by oxidation when hydroperoxide levels increase. We show that Yap1 is not directly oxidized by hydroperoxide. We identified the glutathione peroxidase (GPx)-like enzyme Gpx3 as a second component of the pathway, serving the role of sensor and transducer of the hydroperoxide signal to Yap1. When oxidized by H_2O_2, Gpx3 Cys36 bridges Yap1 Cys598 by a disulfide bond. This intermolecular disulfide bond is then resolved into a Yap1 intramolecular disulfide bond, the activated form of the regulator. Thioredoxin turns off the pathway by reducing both sensor and regulator. These data reveal a redox-signaling function for a GPx-like enzyme and elucidate a eukaryotic hydroperoxide-sensing mechanism. Gpx3 is thus a hydroperoxide receptor and redox-transducer.

Introduction

The concentration of reactive oxygen species (ROS) (hydroperoxides and superoxide anion) is narrowly set by changes in oxidant-scavenging enzymes levels that compensate for the continuous alterations in ROS production rates during growth and impromptu exogenous insults (Gonzalez-Flecha and Demple, 2000). This homeostatic control is essential to preserve cellular integrity. Specialized pathways that detect minimal increases in ROS intracellular concentration regulate this homeostasis, raising the important question of the biochemical mechanisms sensing and translating ROS signals into a coordinated output. Solutions to this question have been provided by the detailed characterization of the prokaryotic OxyR and SoxR transcription factors that sense and transduce hydrogen peroxide (H_2O_2) and superoxide anion signals, respectively (Kim et al., 2002; Pomposiello and Demple, 2001; Zheng et al., 1998).

In budding yeast, the bZip transcription factor Yap1 is a functional homolog of OxyR. Yap1-deleted strains are hypersensitive to H_2O_2 and t-butyl hydroperoxide (t-BOOH) due to their inability to elevate the expression of genes encoding most antioxidants and components of the cellular thiol-reducing pathways (Carmel-Harel et al., 2001; Gasch et al., 2000; Kuge and Jones, 1994; Lee et al., 1999). Yap1 also regulates the stress tolerance to other classes of compounds including the thiol oxidant diamide, the electrophile diethylmaleate, and cadmium (Kuge and Jones, 1994; Vido et al., 2000; Wu et al., 1993). Yap1 is primarily controlled by a redox-sensitive nuclear export regulating its nuclear accumulation upon activation (Delaunay et al., 2000; Kuge et al., 1997, 1998; Yan et al., 1998). Redox signals inhibit Yap1 export by causing modifications of its nuclear export signal (NES). These modifications differ in response to peroxides and diamide (Coleman et al., 1999; Delaunay et al., 2000; Kuge et al., 2001). Upon activation by H_2O_2, Yap1 is oxidized to an intra-molecular disulfide bond between Cys303 and Cys598, with the resulting change of conformation probably masking the Yap1 NES (Delaunay et al., 2000). The close correlation between Yap1 oxidation and activation further indicates that oxidation is the trigger for activation and suggests that Yap1 itself is a component of the cellular mechanism sensing H_2O_2. Activation of Yap1 by diamide does not lead to the formation of the Cys303-Cys598 disulfide bond (Delaunay et al., 2000), but instead to disulfide bonds between C-terminal cysteines C598, C620, and C629 which also probably modify the Yap1 NES (Kuge et al., 2001). Two important questions remain in the actual redox signals that are sensed by the Yap1 pathway and in the molecular events that lead from these signals to Yap1 oxidation.

Here, we demonstrate that Yap1 is not directly oxidized by hydroperoxide. We identify the thiol peroxidase Gpx3 as the hydroperoxide sensor that promotes the oxidation of Yap1 to its intra-molecular disulfide bond, the activated form of the regulator. This function of Gpx3 uncovers a tight coupling between the mechanisms of hydroperoxide sensing and scavenging. Our findings describe a redox-sensing mechanism in a eukaryote involving a receptor-initiated hydroperoxide signaling pathway based on a thiol oxidation cascade.

Results

Yap1 Is Transiently Disulfide-Linked to a 20 kDa Protein upon Activation by H_2O_2

Yap1 is activated by oxidation when cells are exposed to H_2O_2, but the way oxidation occurs is not understood (Delaunay et al., 2000). We analyzed the redox forms of Myc epitope-tagged Yap1 (Myc-Yap1) by Western blot with an anti-Myc antibody. Using the cysteine-trapping method, we previously showed that in H_2O_2-treated cells

[3]Correspondence: toledano@jonas.saclay.cea.fr

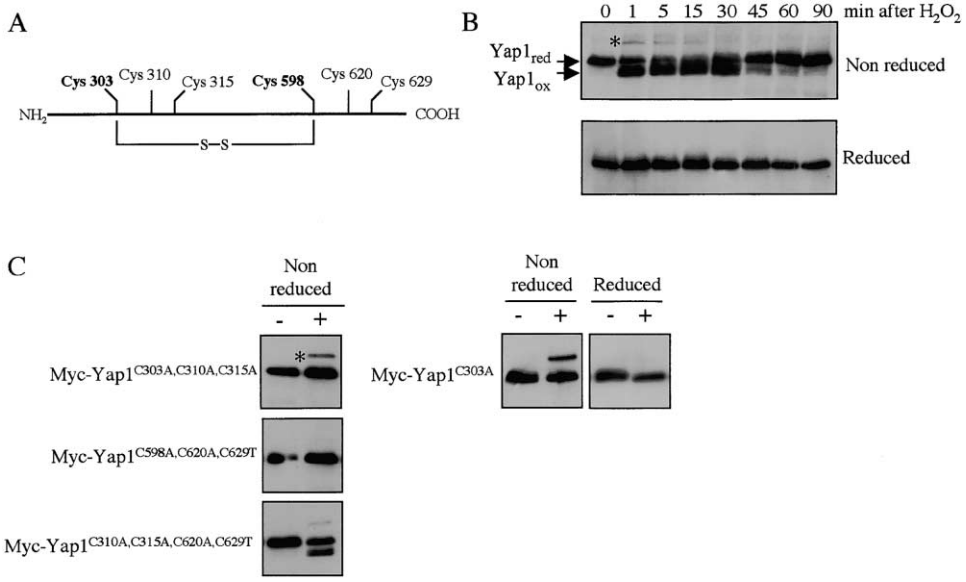

Figure 1. Yap1 Is Transiently Disulfide-Linked to a Small Protein upon Activation by H_2O_2

(A) Schematics of Yap1 depicting its six cysteines residues and intra-molecular disulfide bond.

(B) Analysis of the in vivo Yap1 redox state by an anti-Myc immunoblot. Crude extracts from a Δ*yap1* strain carrying Myc-Yap1, untreated or exposed to H_2O_2 (0.4 mM) during the indicated period were resolved under non-reducing or reducing conditions, as indicated. The Yap1 mixed-disulfide is indicated by an asterisk, and the Yap1 reduced and intra-molecular disulfide forms by arrows.

(C) Effects of Yap1 cysteine mutations on mixed disulfide formation. Extracts from Δ*yap1* strains carrying the indicated Yap1 alleles not treated or exposed for 2 min to H_2O_2 (0.4 mM) were prepared and analyzed as in (B) under non-reducing and reducing conditions as indicated.

Yap1 has a distinct faster mobility than in untreated cells (Delaunay et al., 2000; see Figure 1B). This mobility shift occurs as early as 1 min after H_2O_2 treatment and starts to disappear after 30 min. It is diagnostic of a Cys303-S-S-Cys598 intra-molecular disulfide bond, because it completely disappears upon reduction or when alanine is substituted for either Cys303 or Cys598 (see schematics, Figures 1A and 1C). Further inspection of the autoradiogram revealed a faint anti-Myc stained higher molecular weight (MW) band whose presence correlated with Yap1 oxidation, disappearing after 15 min (Figure 1B). The absence of this band under reducing conditions indicated a probable intermolecular disulfide linkage of a small fraction (<10%) of Yap1 with a protein of about 20 kDa, as predicted from the band migration (Figure 1B). Analysis of Yap1 cysteine mutants showed that the high MW Yap1 band was almost completely erased with an allele carrying substitutions of its three carboxy-terminal cysteines (Yap1$^{C598A, C620A, C629T}$). In contrast, the high MW band was strongly increased with an allele carrying substitutions of its three amino-terminal cysteines (Yap1$^{C303A, C310A, C315A}$) (Figure 1C). Such stabilization of the Yap1 mixed disulfide was also seen in Yap1^{C303A}, with about 30%–50% of the total Yap1 protein involved in this linkage (Figure 1C and see Figure 2A). Notably, the high MW Yap1 band had a wild-type intensity in a Yap1 allele only containing Cys303 and Cys598 (Yap1$^{C310A, C315A, C620A, C629T}$).

The data indicate the transient formation of a Yap1 mixed-disulfide. This linkage presumably involves Cys598 and is stabilized when Cys303 is missing.

The Yap1 Disulfide-Linked Partner Is Glutathione Peroxidase

We purified H_2O_2-treated Myc-Yap1^{C303A} by one-step anti-Myc affinity chromatography under non-reducing conditions. The mixed-disulfide partner copurified with Yap1 under these conditions (Figure 2A). Analysis of the tryptic digest of the Yap1 high MW band by nanoscale capillary liquid chromatography-tandem mass spectrometry (LC-MS/MS) identified Yap1^{C303A} as the first protein candidate (40% sequence coverage) and Gpx3 as the only other protein (27% sequence coverage, peptides 26–35, 96–108, and 142–160) (Figure 2B). The identification of Gpx3 as the Yap1^{C303A} mixed disulfide-linked partner was confirmed by the absence of the high MW band in a *GPX3* deleted strain (Δ*gpx3*) after exposure to hydroperoxide (Figure 2C). Gpx3 is one of the three budding yeast glutathione peroxidases (GPx), which are non-selenium enzymes (Avery and Avery, 2001; Inoue et al., 1999). The Gpx3 theoretical size of 18.5 kDa is in agreement with the predicted size of the Yap1 mixed disulfide partner, indicating that the two proteins form a 1:1 stoichiometric complex. Gpx3 is a constitutively expressed enzyme, and its expression is not altered by oxidative stress or by mutations in *YAP1* (Inoue et al., 1999).

We next tested whether Gpx3 is also the disulfide-linked partner of wild-type Yap1, by a Myc-Yap1 immunoprecipitation from TCA lysates of H_2O_2-induced cells expressing a HA-tagged version of Gpx3 (HA-Gpx3) (Figure 2D). The immunoprecipitated material contained a unique anti-HA stained band that migrated at the size of the anti-Myc stained Yap1 high MW band. A HA-Gpx3

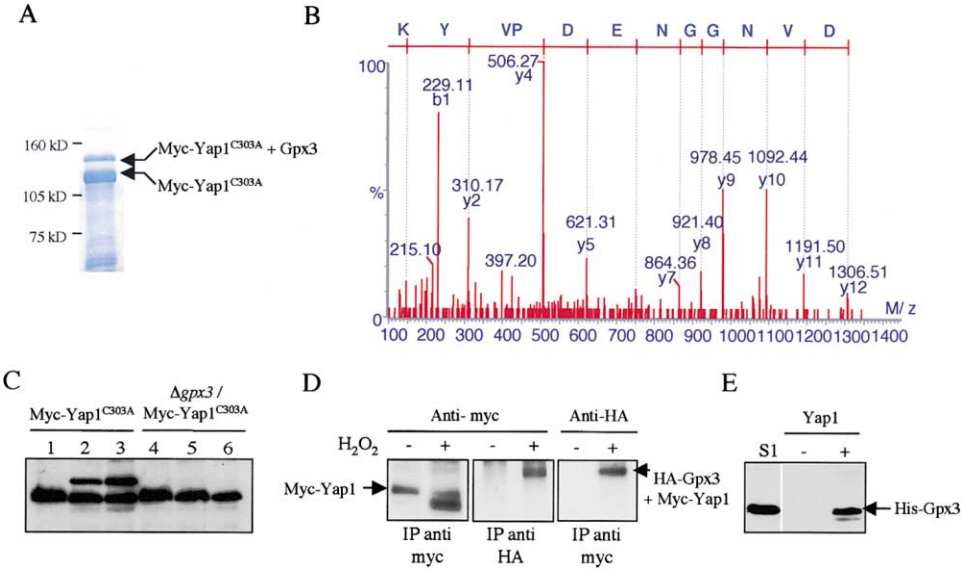

Figure 2. Gpx3 Is the Yap1-Mixed Disulfide Partner

(A) Preparative non-reducing SDS-PAGE of purified Myc-Yap1^{C303A}. The free and mixed-disulfide forms are indicated. Yap1 was purified from extracts of a Δ*yap1* strain carrying Myc-Yap1^{C303A} exposed during 5 min to H_2O_2 (0.6 mM).

(B) Identification of peptide 96–108 of Gpx3 by fragmentation using tandem mass spectrometry. For identification, experimental fragmentation patterns of selected peptides were compared to theoretical values calculated according to the NCBInr database.

(C) The Yap1^{C303} mixed-disulfide is absent in a strain lacking Gpx3. Extracts from Δ*yap1* or Δ*yap1*Δ*gpx3* strains carrying Yap1^{C303A} and left untreated (lanes 1, 4) or exposed during 2 min to H_2O_2 (0.4 mM) (lanes 2 and 5) or t-BOOH (1 mM) (lanes 3 and 6), were prepared and analyzed as in Figure 1B under non-reducing conditions.

(D) The mixed-disulfide partner of wild-type Yap1 is also Gpx3. Yap1 was immunoprecipitated with the anti-Myc Mab (IP anti myc) or with the anti-HA Mab (IP anti HA) from extracts of a Δ*yap1* strain carrying both Myc-Yap1 and HA-Gpx3 and left untreated or exposed to H_2O_2 (0.4 mM) during 2 min. Extracts were prepared as in Figure 1B. The immunoprecipitated material resolved under non-reducing conditions was immunoblotted with either the anti-Myc or anti-HA Mab as indicated.

(E) Reduced Yap1 and Gpx3 interact in a pull-down assay. Extracts from Δ*yap1* strains carrying or not Myc-Yap1, were incubated under reducing conditions (DTT 2 mM) with anti-Myc Mab-bound sepharose beads during 3 hr at 4°C. A low speed supernatant fraction from a lysate of *E.coli* expressing His-Gpx3 (S1) was applied onto the anti-Myc Mab-bound sepharose beads. After iterative washings, the anti-Myc bound material was eluted by competition with an excess Myc peptide and immunoblotted with anti-His Mab after non-reducing SDS-PAGE. The experiment was performed under anaerobiosis.

immunoprecipitation under the same conditions also showed a unique anti-Myc stained band of the size of the high MW band (Figure 2D).

In view of the mixed-disulfide formed by wild-type Yap1 and Gpx3 in H_2O_2-treated cells, we also tested whether these proteins could interact non-covalently under non-induced conditions (Figure 2E). *E. coli*-expressed Gpx3 was specifically retained by Myc-Yap1 that had been immobilized on an anti-Myc immunoaffinity column. This result was obtained both under anaerobiosis with fully reduced proteins (Figure 2E) and under aerobiosis with reduced and then alkylated proteins (not shown).

In summary, these data demonstrate that upon exposure to H_2O_2, Yap1 associates with Gpx3 by a disulfide bridge. A preformed Yap1-Gpx3 non-covalent complex might favor this redox interaction.

Disulfide Linkage between Gpx3 Cys36 and Yap1 Cys598 Leads to Yap1 Oxidation

Inspection of the Yap1 redox state in Δ*gpx3* showed that neither the Yap1 high MW band nor the shift to a faster mobility occurred, up to 90 min after treatment with either H_2O_2 (Figure 3A) or t-BOOH (not shown), establishing that Gpx3 is critical for the oxidation of Yap1 in vivo. We next evaluated if Gpx3 is also required for oxidation of Yap1 by hydroperoxides in vitro (Figure 3B). When H_2O_2 (100 μM) was added to premixed reduced purified Yap1 and *E. coli*-expressed Gpx3, a disulfide bond was formed between the two proteins, and Yap1 became partially oxidized to its faster mobility band in a Gpx3-dependent manner (Figure 3B). Therefore, Gpx3 is also required for Yap1 oxidation by H_2O_2 in vitro, although oxidation is not as efficient as in vivo, maybe due to a missing component of the reaction. At a higher H_2O_2 concentration (400 μM), some oxidation of Yap1 was seen in the absence of Gpx3 (not shown), indicating that the Gpx3 requirement can be bypassed in vitro.

Gpx3 carries three cysteines at positions 36, 64, and 82, with Cys36 being the conserved GPx active site-selenocysteine/cysteine residue (see schematics in Figure 3C). To identify which of these cysteines are required for Yap1 oxidation, we coexpressed Gpx3 cysteine mutants with Myc-Yap1 in Δ*gpx3* (Figure 3C). Upon H_2O_2 treatment of the strain carrying Gpx3^{C36S}, Yap1 formed neither the shift to a faster mobility corresponding to its intra-molecular disulfide form, nor the high MW Gpx3-

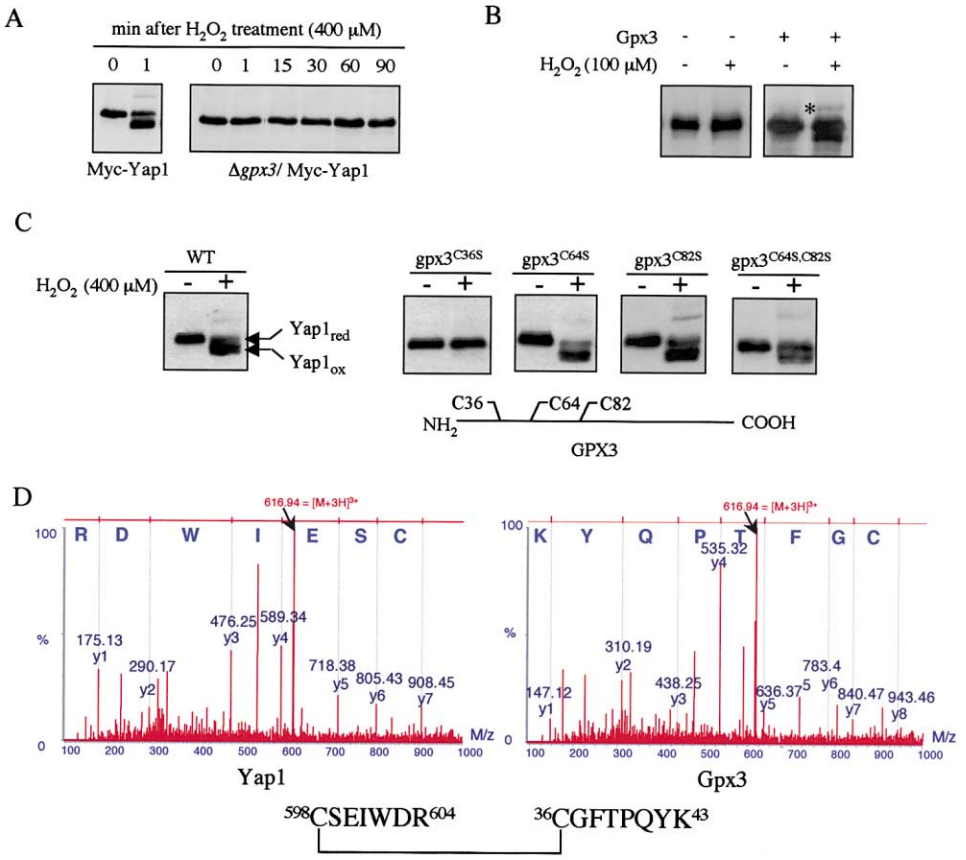

Figure 3. Disulfide Linkage between Gpx3 Cys36 and Yap1 Cys598 Leads to Yap1 Oxidation

(A) Gpx3 is required for in vivo oxidation of Yap1. Δ*yap1* or Δ*yap1*Δ*gpx3* strains carrying Myc-Yap1 were left untreated or exposed to H_2O_2 (0.4 mM) during the indicated period. Extracts were prepared and analyzed under non-reducing conditions as in Figure 1B.

(B) Gpx3 is required for in vitro oxidation of Yap1. H_2O_2 (0.1 mM) was added or not to purified reduced Myc-Yap1 (1 μM) alone or mixed with a 10-fold molar excess of purified reduced Gpx3 as indicated, at room temperature under anaerobiosis. The reaction was stopped by NEM (10 mM) after 10 min and the Yap1 redox state was monitored by immunobloting. The Yap1-Gpx3 mixed-disulfide is indicated by an asterisk. Purified Yap1 and *E. coli*-expressed His-Gpx3 were maintained reduced by overnight incubation in buffer E supplemented with DTT (20 mM), dialyzed against buffer E, under anaerobiosis.

(C) Identification of Gpx3 cysteines required to oxidize Yap1. Δ*yap1*Δ*gpx3* strains carrying Myc-Yap1 and either Gpx3, $Gpx3^{C36S}$, $Gpx3^{C64S}$, $Gpx3^{C82S}$, or HA-$Gpx3^{C64S,\ C82S}$ as indicated, were left untreated or exposed to H_2O_2 (0.4 mM) during 2 min. Inspection of the Yap1 redox state is as in Figure 1B. Shown under the immunoblot is a schematic of Gpx3 depicting its three cysteines.

(D) Identification of the cysteines involved in the mixed-disulfide. The MS/MS spectrum of the fragmentation of the Yap1-Gpx3 disulfide-linked peptide (MW = 1847.82 Da) is interpreted twice according to the sequence of either of its Yap1 or Gpx3 constituting peptides. The base peak (m/z = 616.94 Da) corresponds to the triply charged precursor.

mixed disulfide. In contrast, in strains carrying $Gpx3^{C64S}$, $Gpx3^{C82S}$, or $Gpx3^{C64S,C82S}$, oxidation of Yap1 occurred normally (Figure 3C) and with wild-type kinetics (not shown). Thus, Cys36 is uniquely required for Yap1 oxidation, probably forming the mixed disulfide with Yap1 Cys598 as suggested above. To confirm the identity of the mixed-disulfide linked cysteines, we performed a nanoESI-Q-TOF MS/MS analysis of the non-reduced $Yap1^{C303A}$-Gpx3 sample shown in Figure 2A. An ion with a mass matching the theoretical mass of a disulfide linkage between peptides 598–604 of Yap1 and 36–43 of Gpx3 was detected in the tryptic digest. Fragmentation of this peptide by MS/MS formally identified the Yap1 and Gpx3 expected sequences (Figure 3D). The free Yap1 Cys598 and Gpx3 Cys36-containing peptides were not detected in this sample, indicating that the mixed disulfide could not involve another Yap1 cysteine, unless a second disulfide bond was bridging Yap1 and Gpx3. However, the normal Yap1-Gpx3 mixed-disulfide bond formation and Yap1 oxidation observed with $Gpx3^{C64S,C82S}$ rules out this possibility. MS analysis of the same material after reduction and alkylation by iodoacetamide showed the disappearance of this mixed disulfide and the appearance of its two constitutive peptides (not shown).

These data establish that the H_2O_2-induced $Yap1^{C303A}$-Gpx3 mixed disulfide is formed between Cys598 and Cys36. The same residues are probably bridging Yap1 with Gpx3 in the wild-type context, although in the absence of Yap1 Cys598, another probably illegitimate inter-molecular disulfide bond forms (see Figure 1C). Moreover, formation of the Yap1-Gpx3 mixed disulfide bond is essential for the generation of the Yap1 intramolecular disulfide bond.

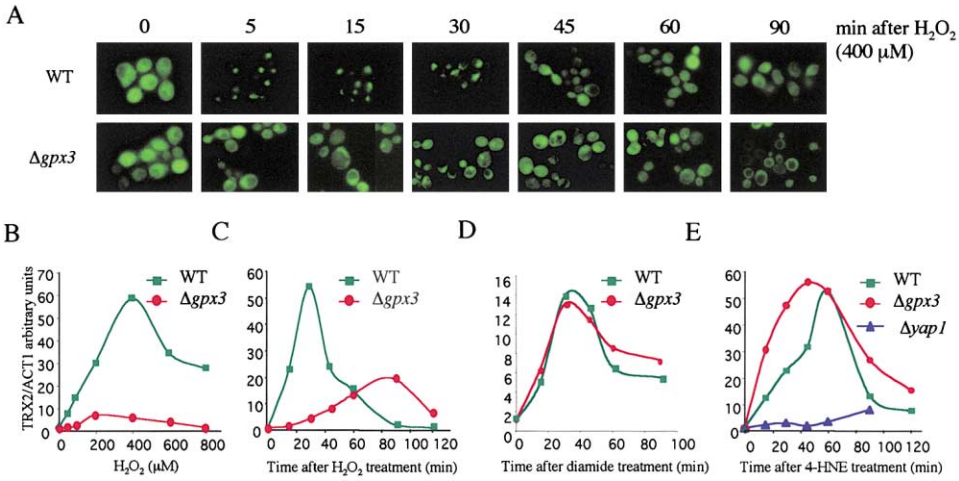

Figure 4. Gpx3 Is Exclusively Required for Yap1 Activation by Hydroperoxides

(A) Analysis of the GFP-Yap1 cellular localization. Exponentially growing wild-type or Δ*gpx3* strains carrying GFP-Yap1 were treated with H_2O_2 (0.4 mM) during the indicated period and analyzed for GFP staining as described (Delaunay et al., 2000).

(B) Dose-response of *TRX2* induction. Total RNA was extracted from wild-type and Δ*gpx3* left untreated or exposed during 30 min at the indicated H_2O_2 concentration. *TRX2*/*ACT1* mRNA ratios were quantified by on-line RT-PCR.

(C) Kinetics of *TRX2* induction. Wild-type and Δ*gpx3* cells were exposed to H_2O_2 (0.4 mM) during the indicated period.

(D) Wild-type and Δ*gpx3* were exposed to diamide (1.5 mM) during the indicated period and *TRX2* induction measured as in (B).

(E) Wild-type, Δ*gpx3*, and Δ*yap1* cells were exposed to 4-HNE (250 μM) during the indicated period and *TRX2* induction measured as in (B).

Gpx3 Is Exclusively Required for the Activation of Yap1 by Hydroperoxides

Oxidation of Yap1 by peroxides triggers its nuclear redistribution and its ability to activate target-gene expression (Delaunay et al., 2000). In Δ*gpx3*, a GFP-Yap1 fusion remained mainly cytoplasmic up to 90 min after H_2O_2 treatment, in contrast to its exclusive nuclear localization in the wild-type strain during the first 30 min of this treatment (Figure 4A). Nevertheless, a few cells (10%–30%) showed a very partial GFP-Yap1 staining in the nucleus in Δ*gpx3* after 30 min, demonstrating that Yap1 nuclear redistribution, although significantly inhibited, could still occur. In Δ*gpx3* cells, induction of the Yap1 target-gene *TRX2* measured after 30 min of treatment was defective through a range of H_2O_2 concentration from 50 to 800 μM (Figure 4B). Furthermore, *TRX2* induction was delayed by an hour and significantly diminished in Δ*gpx3* in comparison to the wild-type kinetics (Figure 4C). This residual *TRX2* induction is dependent upon Yap1 since it was absent in Δ*gpx3*Δ*yap1* strain (not shown). Yap1 is also activated by diamide through a mechanism not involving the C303-S-S-C598 bond formation (Delaunay et al., 2000), and by electrophiles that supposedly operate by covalent modification of Yap1 C-terminal cysteines (D.A., A.D., C. R.-P., F.T. and M.B.T, unpublished data). We thus evaluated whether Gpx3 was also required for activation of Yap1 by these compounds. *TRX2* was fully induced by diamide irrespective of the presence of Gpx3 (Figure 4D). *TRX2* was also induced in a Yap1-dependent manner by the electrophile by-product of lipid peroxidation, 4-hydroxynonenal (4-HNE) irrespective of the presence of Gpx3 (Figure 4E). Gpx3 is thus exclusively required for Yap1 activation by hydroperoxide. The Gpx3-independent Yap1 activation by 4-HNE and diamide provides an explanation for the residual, hydroperoxide-induced Yap1 activation occurring in the absence of Gpx3. In this case, secondary oxidation by-products generated by hydroperoxide might trigger the Gpx3-independent Yap1 activation mechanism.

The Gpx3 Peroxidase Function Involves an Active-Site Disulfide

The Yap1 hydroperoxide sensor Gpx3 is a previously identified hydroperoxide scavenger. It was thus important to determine whether different Gpx3 cysteine residue(s) operate in its different functions.

We analyzed the redox forms of HA-Gpx3 with the procedure used for the analysis of Yap1. In untreated cells, HA-Gpx3 migrated as a single band, but in cells treated with H_2O_2, a second faster mobility band was apparent (Figure 5A). This faster band was diagnostic of a Cys36-S-S-Cys82 disulfide bond because it was seen neither under reducing conditions nor in Gpx3 cysteine mutants $Gpx3^{C36S}$ or $Gpx3^{C82S}$. An MS/MS analysis by nanoESI-Q-TOF of the chymotryptic digest of *E. coli*-expressed oxidized Gpx3 confirmed the presence of this disulfide bond (not shown). We tested the significance of this disulfide bond by assaying in vitro the peroxidase activity of purified *E. coli*-expressed Gpx3 and its cysteine substitution derivatives (Figure 5B). Gpx3 had a significant peroxidase activity in the presence of thioredoxin and thioredoxin reductase (see below). In contrast, $Gpx3^{C82S}$ did not have any detectable peroxidase activity (Figure 5B), indicating that the Gpx3 intra-molecular Cys36-S-S-Cys82 disulfide is essential for the peroxidase catalytic mechanism.

The Yap1 Regulatory Role of Gpx3 Is Prevalent over its Peroxidase Function

The respective in vivo hydroperoxide sensing and scavenging Gpx3 functions were evaluated. We confirmed

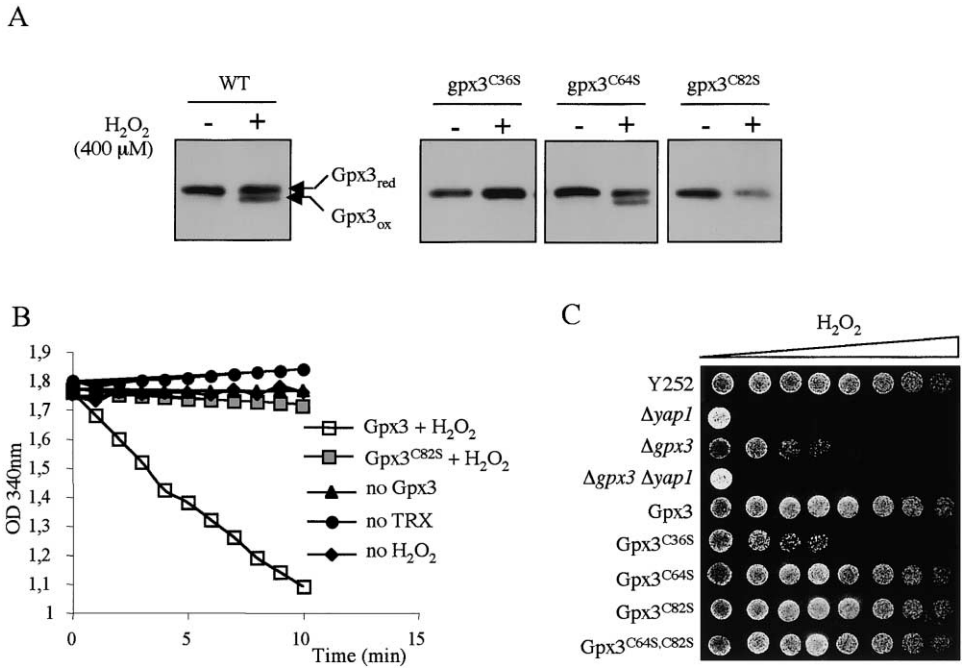

Figure 5. The Gpx3 Peroxidase Catalytic Mechanism Involves an Active-Site Disulfide

(A) In vivo analysis of the Gpx3 redox state. NEM-blocked extracts from Δ*gpx3* carrying HA-Gpx3, HA-Gpx3^{C36S}, HA-Gpx3^{C64S}, or HA-Gpx3^{C82S} left untreated or exposed to H_2O_2 (0.4 mM) for 2 min were prepared as described in methods, and immunoblotted with an anti-HA Mab after non-reducing SDS-PAGE.

(B) Gpx3 peroxidase assays. The complete assay in the presence of Gpx3, thioredoxin, thioredoxin reductase, NADPH, and H_2O_2 (open squares). Complete reaction with Gpx3 C82S replacing Gpx3 (gray squares). Complete reaction without Gpx3 (filled triangles). Complete reaction without thioredoxin (filled circles). Complete without H_2O_2 (filled diamonds). Data are expressed as the decrement of the O.D. = 340 nm over time.

(C) Plate hydroperoxide sensitivity assays. Δ*gpx3*, Δ*yap1*, Δ*yap1*Δ*gpx3*, or Δ*gpx3* carrying pRS316-HA-Gpx3 or the indicated Gpx3 cysteine mutants were grown in CASA medium to stationary phase and spotted on medium containing increasing H_2O_2 concentrations (0.4 to 2.5 mM). Growth was inspected after three days at 30°C.

the previously reported decreased tolerance of Δ*gpx3* toward hydroperoxides (Avery and Avery, 2001; Inoue et al., 1999) (Figure 5C). However, this phenotype, previously attributed to a defective peroxidase activity, could be caused by the defective Yap1 activation, or by both defects. We thus took advantage of Gpx3 mutants that uncouple its two functions. While Cys36 is required for both Yap1 activation and hydroperoxide reduction, Cys82 is only required for the latter function. A Δ*gpx3* strain carrying Gpx3^{C36S} was as sensitive to H_2O_2 as the Δ*gpx3* strain. However a Δ*gpx3* strain carrying either Gpx3^{C64S}, or Gpx3^{C82S}, or Gpx3^{C64S,C82S} had a wild-type tolerance to hydroperoxides (Figure 5C). These data suggest that the hydroperoxide phenotype of Δ*gpx3* is primarily due to defective Yap1 activation. Tolerance assays also showed that the Δ*gpx3* strain, although hypersensitive to H_2O_2, was more resistant than the Δ*yap1* strain. However, when *YAP1* was deleted in Δ*gpx3*, the resulting strain (Δ*yap1*Δ*gpx3*) was as sensitive as Δ*yap1*, indicating that the higher H_2O_2 tolerance of Δ*gpx3* is due to Yap1 and might relate to the Gpx3-independent activation mechanism suggested above.

Gpx3 Is Reduced by Thioredoxin and not by GSH

Our data, by showing that Gpx3 oxidizes Yap1, imply that their redox states are coupled. However, this is seemingly contradictory with the exclusive coupling of Yap1 to thioredoxin (Carmel-Harel et al., 2001; Delaunay et al., 2000; Izawa et al., 1999) and the purported coupling of Gpx3 to GSH (Avery and Avery, 2001). We thus evaluated the GSH dependence of Gpx3 by comparing its in vivo redox state in a wild-type and in isogenic strains with inactivation of either thiol reducing pathways. To better monitor Gpx3 oxidation, we increased the separation of its reduced and disulfide forms by alkylating free thiol groups with the high molecular mass alkylating agent AMS. In reduced Gpx3, Cys36, Cys64, and Cys82 are available for alkylation by AMS (3 × 0.5 kDa) whereas in oxidized Gpx3, only Cys64 is available (0.5 kDa). This differential alkylation, by giving a further 1 kDa difference between reduced and oxidized bands, clearly indicated that fully reduced Gpx3 became about half-oxidized as early as 2 min after exposure to H_2O_2 and was then reduced after 15 min (Figure 6A), closely paralleling the occurrence of the Yap1-Gpx3 mixed disulfide (see Figure 1A). The GSH pathway was tested in a strain lacking the glutathione reductase gene *GLR1* (Δ*glr1*) or in Δ*glr1*Δ*gsh1PRO2-1* (Spector et al., 2000). The latter strain lacks both *GLR1* and γ-glutamyl cysteine synthase (*GSH1*), but still carries approximately 0.5% of the WT cellular GSH content. In both strains, the redox state of Gpx3 before and after treatment with H_2O_2 had a wild-type pattern (Figure 6A). In contrast,

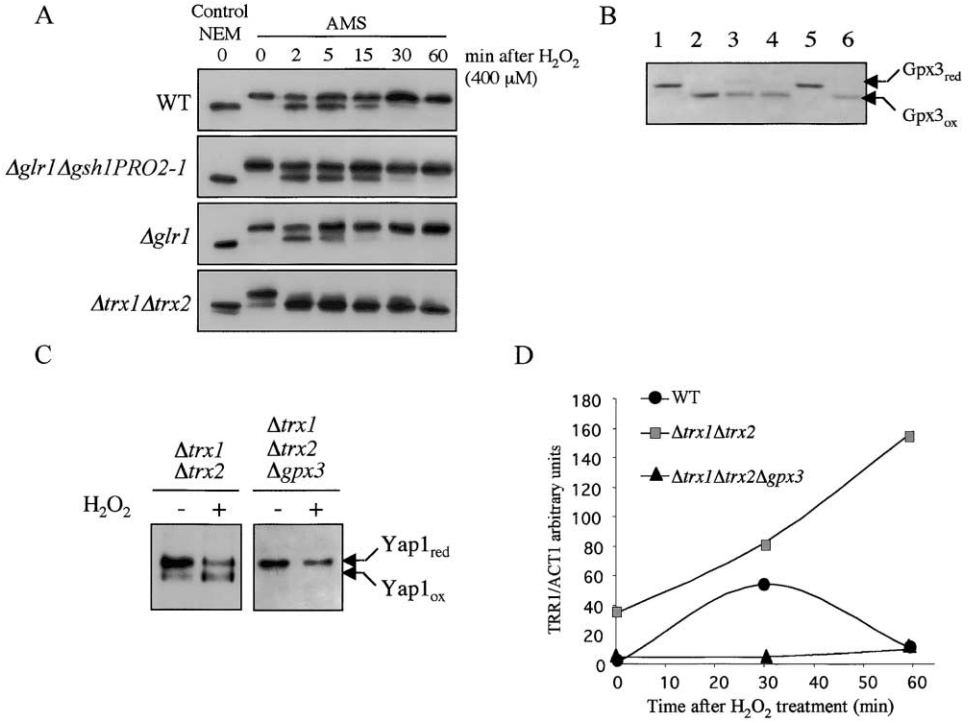

Figure 6. Gpx3 Is Reduced by the Thioredoxin Pathway

(A) The Gpx3 redox state in thiol redox pathways mutants. Wild-type, Δ*glr1*Δ*gsh1PRO2-1*, Δ*glr1*, and Δ*trx1*Δ*trx2* carrying pRS316-HA-Gpx3 were left untreated or were exposed to H_2O_2 (0.4 mM) for the indicated period. TCA precipitated proteins were dissolved in the presence of NEM or AMS as indicated.

(B) In vitro reduction of Gpx3. Ponceau staining of blotted recombinant Gpx3 after separation under non-reducing conditions. Reduced Gpx3 alone (lane 1). Oxidized Gpx3 (lane 2). Oxidized Gpx3, GSH, glutathione reductase, and NADPH (lane 3). Oxidized Gpx3, glutathione reductase, and NADPH (lane 4). Oxidized Gpx3, thioredoxin, thioredoxin reductase, and NADPH (lane 5). Oxidized Gpx3, thioredoxin reductase, and NADPH (lane 6). Recombinant reduced Gpx3 (25 μM) oxidized by H_2O_2 (0.25 mM) was incubated with GSH (0.3 mM), glutathione reductase (2 μM), thioredoxin (20 μM), thioredoxin reductase (1 μM), and NADPH (0.3 mM) in a 20 μl final volume for 10 min at 30°C. The reaction was interrupted by NEM (10 mM) and analyzed by non-reducing SDS-PAGE.

(C) In vivo Yap1 redox state in thioredoxin pathway mutants. Extracts from Δ*trx1*Δ*trx2* or Δ*trx1*Δ*trx2*Δ*gpx3* carrying Myc-Yap1 were left untreated or were exposed to H_2O_2 (0.4 mM) for 2 min and processed as in Figure 1B. Samples were separated under non-reducing conditions.

(D) Gpx3 mediates Yap1 deregulation in thioredoxin mutants. Total RNA was extracted from wild-type, Δ*trx1*Δ*trx2* and Δ*trx1*Δ*trx2*Δ*gpx3* cells exposed to H_2O_2 (0.4 mM) for the indicated period. Induction of *TRR1* was measured as in Figure 4B.

in a strain lacking both cytoplasmic thioredoxin genes *TRX1* and *TRX2* (Δ*trx1*Δ*trx2*), Gpx3 was constitutively partially oxidized (about 10%), and became fully oxidized by H_2O_2 for up to one hour. We confirmed this in vivo observation by assaying the Gpx3 peroxidase activity in vitro. This activity was significant with thioredoxin and thioredoxin reductase as the reducing system (see above, Figure 5B), but undetectable with glutathione reductase and GSH (not shown). We also assayed the reduction of Gpx3 in vitro. Recombinant Gpx3 oxidized by H_2O_2 (Figure 6B, lane 2) was completely reduced by the thioredoxin system (lane 5), but only minimally by the GSH system (lane 3), as shown by its distinct electrophoretic redox forms (Figure 6B). These data establish that thioredoxin and not GSH is the physiological electron donor system for Gpx3.

Gpx3 Mediates the Deregulation of Yap1 in Thioredoxin Mutants

Yap1 is deregulated in strains with an inactivated thioredoxin pathway (Carmel-Harel et al., 2001; Delaunay et al., 2000; Izawa et al., 1999; see also Figure 6D), suggesting that thioredoxin is required for Yap1 reduction, and/or that its absence promotes Yap1 activation. With the above-demonstrated essential requirement of Gpx3 for Yap1 oxidation and activation, we tested whether Gpx3 could mediate the deregulation of Yap1 in thioredoxin pathway mutants. We thus deleted *GPX3* in a strain lacking both thioredoxin genes (Δ*trx1*Δ*trx2*Δ*gpx3*) (Figures 6C and 6D). In contrast to its partial constitutive oxidation seen in Δ*trx1*Δ*trx2*, Yap1 was fully reduced in Δ*trx1*Δ*trx2*Δ*gpx3* and did not oxidize upon H_2O_2 treatment (Figure 6C). Similarly, the constitutive and unregulated H_2O_2 induction of the Yap1-target gene *TRR1*, seen in Δ*trx1*Δ*trx2*, was suppressed in the triple deleted strain (Figure 6D). Hence, Gpx3 is also essential for the constitutive partial activation of Yap1 in thioredoxin pathway mutants.

Discussion

We have identified Gpx3 as the hydroperoxide sensor of the Yap1 pathway. Gpx3, hitherto known as a thiol peroxidase, is shown to perceive intracellular hydroper-

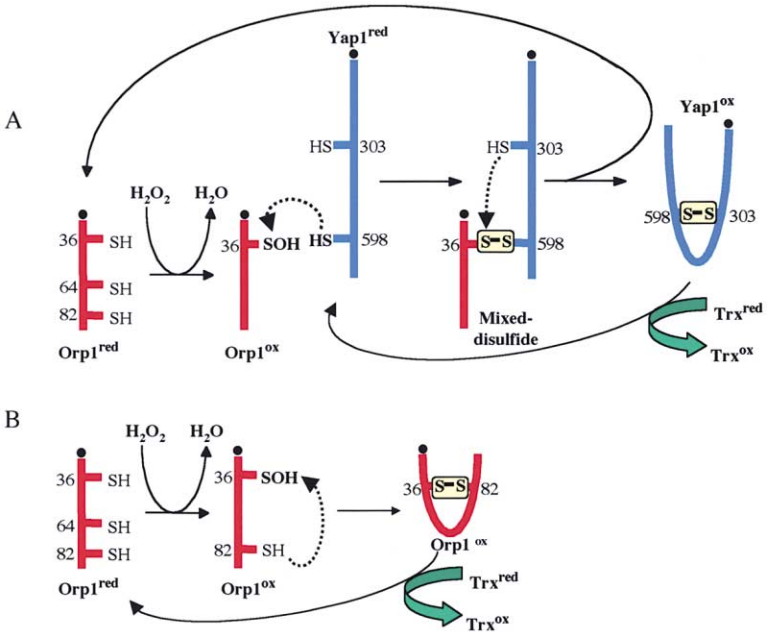

Figure 7. A Working Model Depicting the Dual Hydroperoxide Sensing and Scavenging Functions of Orp1/Gpx3

Two pools of Orp1/Gpx3 exist, (A) one in a pre-complex with Yap1 and serving the hydroperoxide sensing function, and (B) the other, either free in the cell or perhaps membrane bound, serving the hydroperoxide scavenging function. Sensing involves the peroxidatic reaction of Orp1 Cys36 with hydroperoxides to yield ROH and a sulfenic acid Cys36-SOH. Cys36-SOH then reacts with Yap1 Cys598 to form the Orp1-Yap1 disulfide linkage, followed by its conversion to the intra-molecular Cys303-S-S-Cys598 disulfide of activated Yap1 and the recycling of the Orp1 reduced form. During this cycle, Yap1 reduces Orp1, whereas the former is reduced by thioredoxin. The peroxidase function also involves the peroxidatic reaction of Orp1 Cys36 with hydroperoxides yielding a Cys36-SOH that condensate with the Orp1 Cys82 thiolate to form the intra-molecular Cys36-S-S-Cys82 bridge. Reduction of Orp1 by thioredoxin allows for the efficiency of hydroperoxide scavenging.

oxide levels and to transduce this signal to Yap1 by virtue of specific thiol oxidation. This function of Gpx3 can be easily conceived in view of its thiol peroxidase structure endowed with high hydroperoxide reactivity, thus highlighting a previously unrecognized coupling between hydroperoxide scavenging and sensing. The data presented elucidate a hydroperoxide sensing and signaling pathway based on a thiol oxidation cascade in a eukaryote and stress the high specificity of thiol oxidation reactions in vivo. In this pathway, Gpx3 actually functions as a highly specific hydroperoxide receptor transducing the redox signal to downstream protein thiols. We propose changing the name of Gpx3 to "Oxidant Receptor Peroxidase 1" (Orp1).

Upon exposure to H_2O_2 or t-BOOH, Yap1 Cys598 and Orp1 Cys36 transiently form an inter-molecular disulfide linkage essential for oxidation and activation of Yap1. This is demonstrated by the in vivo and in vitro defective hydroperoxide-induced oxidation of Yap1 in the absence of Orp1, further indicating that Orp1 is the peroxide receptor of the Yap1 pathway. The exclusive requirement of Orp1 Cys36 in Yap1 activation (Figure 3C) indicates that this cysteine is the site of peroxide sensing, agreeing with it being the conserved peroxidase active-site residue. We propose the following model of how Orp1 senses hydroperoxide and oxidizes Yap1 (Figure 7). Orp1 Cys36 is directly oxidized by H_2O_2 to yield H_2O and a sulfenic acid Cys36-SOH, the expected oxidation product of a cysteine residue by hydroperoxides (Claiborne et al., 1999; Ellis and Poole, 1997). The nascent Cys36-SOH reacts with Yap1 Cys598 to form the Orp1-Yap1 disulfide linkage. This Yap1-Orp1 inter-molecular disulfide linkage is then transposed to the intramolecular C303-S-S-C598 disulfide of activated Yap1 with recycling of reduced Orp1. The thiol-disulfide exchange reaction probably results from a nucleophilic attack of the mixed-disulfide bond by Yap1 Cys303A, as suggested by stabilization of the inter-molecular disulfide bond in $Yap1^{C303A}$. This is the simplest model that fits the experimental data. One of the in vivo oxidized forms of Orp1 contains a Cys36-S-S-Cys82 intra-molecular disulfide bond (Figure 5A) that could also oxidize Yap1 by a mechanism of thiol-disulfide exchange reaction. Although this possibility cannot be formally excluded, the existence of two mechanisms of oxidation is unlikely. The proposed model thus supposes that when formed, the Cys36 sulfenic acid is poised to react with either Yap1 Cys598 or Orp1 Cys82. Yet, mixed disulfide bond formation might be favored at the expense of the Orp1 intra-molecular disulfide, if a pool of Orp1 is in a pre-complex with Yap1, as suggested by their in vitro non-covalent interaction (Figure 2E). Such a model describes a two-components system for sensing and transducing the hydroperoxide signal thus distinguishing four cysteines (Cys36, Cys82, Cys303, and Cys598), each carrying a unique redox reactivity. As the sensor, Orp1 Cys36 is endowed with high hydroperoxide reactivity, which might relate to high nucleophilicity, low pKa value, and the ability to stabilize the RO^--leaving group of the peroxide substrate by a proton-donating group (Ellis and Poole, 1997). The Cys36 amino acid environment probably determines its unique reactivity. The three other cysteines must have both a high nucleophilicity and a much lower reactivity toward peroxides.

As presented, the proposed model addresses the mechanism of Yap1 oxidation by hydroperoxide, but not its reduction. Based on genetic and biochemical data, both Yap1 (Carmel-Harel et al., 2001; Delaunay et al., 2000; Izawa et al., 1999) and Orp1 (Figure 6) redox states are coupled to the thioredoxin pathway. The above model also postulates that the redox states of Yap1 and Orp1 are coupled, suggesting that Orp1 could reduce oxidized Yap1 with electrons from thioredoxin, in addition to oxidizing it. The Orp1-Yap1 disulfide linkage, which starts resolving 15 min after exposure to H_2O_2 at the outset of Yap1 reduction (see Figure 1A), is compati-

ble with this hypothesis. However, in vitro, thioredoxin and not Orp1 is capable of reducing oxidized Yap1 (Delaunay et al., 2000; and data not shown), which favors a separate reduction of Yap1 and Orp1 by the thioredoxin pathway.

Function of Orp1 as a Dual Peroxide Sensor and Scavenger

Orp1 was identified as one of the three yeast GPxs that encode a cysteine residue at the conserved active site instead of a selenocysteine most commonly found in other GPxs (Inoue et al., 1999). All three yeast enzymes resemble more the phospholipid hydroperoxide glutathione peroxidases (PHGPx) subfamily, based on their sequence and substrate specificity that includes H_2O_2, t-BOOH, and hydroperoxides esterified to phospholipids (Avery and Avery, 2001). They also share with PHGPxs two gaps at similar positions that correspond to dimerization and tetramerization interfaces in other GPxs (Ursini et al., 1995), suggesting that, as PHGPx, the yeast GPxs are monomeric. Our data suggest the following model of peroxide reduction by Orp1, unusual for a GPx-like enzyme. The reduction of hydroperoxide by the active-site cysteine thiolate Cys36 leads to a cysteine sulfenic acid Cys-SOH that reacts with Cys82 to generate an active-site intra-molecular Cys36-S-S-Cys82 disulfide bond, which is then reduced by thioredoxin (see Figure 7). This mechanism is similar to the peroxiredoxin catalytic mechanism (Chae et al., 1994; Ellis and Poole, 1997) and contrasts with the current GPx catalytic model involving hydroperoxide oxidation of the active site-selenocysteine/cysteine residue to a selenic/sulfenic acid and its reduction by GSH (Ursini et al., 1995). The finding of thioredoxin as the Orp1 physiological electron donor system is not unprecedented in GPx family enzymes (Bjornstedt et al., 1994) and not surprising in view of the predicted structure of PHGPx (Ursini et al., 1995) and hence of Orp1. Indeed, both enzymes lack the basic residues of cytosolic GPx that contribute to the orientation of GSH to the peroxidase active site.

Among the three yeast enzymes, Orp1/Gpx3 was reported as the major PHGPx, on the basis of the effect of its deletion on the tolerance to peroxides (Avery and Avery, 2001; Inoue et al., 1999) and of its higher activity toward phospholipid hydroperoxides in vitro (Avery and Avery, 2001). However, one question arising from our study is the actual in vivo contribution of Orp1 to hydroperoxide scavenging. Indeed, our data attribute most if not all the hydroperoxide hypersensitive phenotype of the Δ*orp1* strain to the defective regulatory function of Orp1 in Yap1 activation (see Figure 5). In addition, the observed low constitutive expression and lack of inducibility of Orp1 (Gasch et al., 2000; Inoue et al., 1999), also predicts a limited in vivo hydroperoxide scavenging function for this enzyme, contrasting with other yeast thiol peroxidases, including Gpx2, that are induced by oxidative stress (Gasch et al., 2000; Lee et al., 1999). Nevertheless, the in vivo negligible H_2O_2 and t-BOOH scavenging function of Orp1 observed in this study does not rule out an important activity toward hydroperoxides esterified to phospholipids in membranes, as suggested by in vitro assays (Avery and Avery, 2001).

Orp1 Is a Sensor and Transducer of the Hydroperoxide Signal

Orp1 is identified as both a hydroperoxide sensor and redox transducer of the Yap1 pathway. Hence, after the prokaryotic regulator OxyR (Kim et al., 2002; Zheng et al., 1998), Orp1 is an example of a hydroperoxide-sensing mechanism that relies on the peroxidatic reaction of a highly reactive thiol, which now appears as a universal mechanism. Nevertheless, the yeast hydroperoxide-sensing system differs fundamentally from its prokaryotic counterpart as involving a two-component mechanism instead of one, thus restricting the hydroperoxide Yap1 response to an on-off switch, in contrast to the graded response proposed for OxyR (Kim et al., 2002). The redox-transducing activity of Orp1 establishes the function of a thiol oxidase for a PHGPx-like enzyme. This function appears highly specific, based on preliminary experiments indicating that potential Orp1 thiol oxidase substrates might be present in addition to Yap1 but in a very limited number. Such thiol oxidase activity has been suspected for mammalian PHGPxs, based on their more "opened" structure relative to other GPxs allowing to react with thiols in bulky molecules other than GSH, thus conferring the potential for a diversified substrate specificity (Brigelius-Flohe, 1999; Ursini et al., 1995, 1997). The finding that PHGPx switches its function during sperm maturation from a soluble active peroxidase to an inactive oxidatively cross-linked form indicates a structural role in the capsule of sperm mitochondria (Ursini et al., 1999). This observation also suggests that PHGPx could oxidize specific sperm protein thiols in the presence of hydroperoxides (Godeas et al., 1997; Maiorino et al., 1999). These examples, and the elucidation of the redox signaling function of Orp1, suggest a more widespread usage of selenol/thiol PHGPxs as general hydroperoxide receptors that funnel oxidizing equivalents into diverse thiol redox-based pathways. Further, the very high hydroperoxide reactivity of PHGPx, especially the selenol enzymes, relative to other cellular thiols, suggests that protein thiol oxidation in redox-based signal pathways might be uniquely initiated by such hydroperoxide receptors.

Experimental Procedures

Strains and Growth Conditions

The *S. cerevisiae* strain YPH98 (Sikorski and Hieter, 1989) (*MATa, ura3-52, lys2-801^{amber},* and *ade2-101^{ochre} trp1-Δ1 leu2-Δ1*) and isogenic derivatives were used in all experiments. The Δ*yap1*, Δ*glr1*, Δ*trx1*Δ*trx2*, and Δ*glr1*Δ*gsh1PRO2-1* were previously described (Lee et al., 1999; Spector et al., 2000). The Δ*gpx3*, Δ*yap1*Δ*gpx3*, and Δ*trx1*Δ*trx2*Δ*gpx3* were derived from wild-type, Δ*yap1::LEU2*, Δ*trx1::URA3*Δ*trx2::KAN* strains respectively by replacing the entire *GPX3* ORF with *TRP1* or *KAN*. Cells were grown at 30°C in YPD [1% yeast extracts, 2% bactopeptone, and 2% glucose] or CASA medium [0.67% yeast nitrogen base, 0.1% casaminoacids, and 2% glucose].

Constructs

Myc-Yap1, a N-terminal Yap1 fusion with a 9 Myc epitope, its mutant alleles, and the GFP-Yap1 fusion were previously described (Delaunay et al., 2000; Kuge et al., 1997). A DNA fragment comprising the *GPX3* ORF flanked by 400 bp upstream and 210 bp downstream sequences was PCR-amplified and cloned into the BamHI site of pRS316. The *GPX3* mutant carrying cysteine to serine substitution were created by a two-steps PCR amplification method. The N-ter-

minal HA-Gpx3 fusion, cloned in the Kpn1 site of pRS316 (pRS316-HA-Gpx3), was constructed by a two-steps PCR amplification procedure with oligonucleotides containing the HA epitope sequence: 5′-TGACGTCCCGGACTATGCAGGATCCTATCCATATGACGTTCCAGATTACGCTGCTCAGTGCTCAGAATTCTATAAGCTAGC and 5′CTGCATA**gtccgggacgtcatacggatagcccgcatagtcaggaacatcgtatgggtaaaagatCAT**gataaacttgaatactttac. HA-Gpx3 cysteine mutants were constructed by replacing the EcoRI-EcoRI fragment of pRS316-HA-Gpx3 with the corresponding mutagenized sequence of pRS316-Gpx3 derivatives. Pet28a-His-Gpx3 was constructed by subcloning *GPX3* into the BamHI and XhoI sites of Pet28a, placing the His tag at the N terminus of Gpx3.

Protein Extracts, Electrophoretic Analysis, and Protein Purifications

For analysis of the in vivo Yap1 redox state, extracts were prepared by the TCA acid lysis method as described (Delaunay et al., 2000). Extracts were resolved by non-reducing or reducing 8% SDS-PAGE as indicated and analyzed by immunoblotting with the anti-Myc Mab (9E10). For analysis of the Gpx3 redox state, cultures were stopped by adding TCA (20% final) and lysed by TCA acid lysis. Precipitated proteins were solubilized in the presence of either NEM (N-ethylmaleimide) (50 mM) or AMS (10 mM) (4-acetamido-4'-maleimidylstilbene-2,2'-disulfonic acid) (Molecular Probe), as indicated in the figure legends. Extracts were separated by non-reducing or reducing 15% SDS-PAGE as indicated. For purification of $Yap1^{303A}$, Δ*yap1* carrying pRS-316-Myc-$Yap1^{303A}$ grown to late exponential phase, was exposed to H_2O_2 (0.6 mM) during 5 min, pelleted, washed with NEM (10 mM), and lysed in a French press in buffer L (Tris-Cl [pH 8] [100 mM], NaCl [50 mM], 0.2% Deoxycholate, 0.15% NP-40, and NEM [50 mM]). Extracts were dialyzed against buffer D (Tris-Cl [pH 8] [100 mM], NaCl [50 mM], and 0.15% NP-40) and incubated overnight at 4°C with anti-Myc Mab-bound sepharose beads. Bound proteins were eluted in buffer E (Tris-Cl [pH 8] [50 mM], NaCl [50 mM] with a synthetic Myc peptide [2 μg/μl]). Eluted protein were resolved on a non-reducing 8% SDS-PAGE and stained by colloidal Coomassie blue (Bio-Rad). For in vitro reconstitution assays, Yap1 was purified from cells carrying pRS426-Myc-Yap1 after lysis in a French press in buffer D, supplemented with DTT (1 mM). Purification proceeded as for $Yap1^{303A}$. For purification of recombinant Gpx3, *E. coli* strain BL21 (DE3) (Invitrogen), carrying Pet28a-His-Gpx3 was grown at 37°C in Terrific Broth (bacto-tryptone [12 g/l], yeast extract [24 g/l], glycerol [0.4%], KH_2PO_4 [1.15 g/l], K_2HPO_4 [6.25 g/l], and kanamycin [40 mg/l]) to $OD_{600nm} = 0,5$, induced for 2 hr with isopropyl β-D-thiogalactopyranoside (1 mM), resuspended in lysis buffer (Tris-Cl [pH 8] [100 mM], NaCl [50 mM], DTT [20 mM], and PMSF [1mM]), and lysed by three freeze-thaw cycles followed by sonication. Extracts were clarified by centrifugation (20,000 g, 4°C), and incubated one hour with Ni-NTA agarose beads (Qiagen). The beads were washed with Buffer E supplemented with imidazole (50 mM) and bound proteins were eluted with imidazole (500 mM). For the Yap1 pull-down assay, *E. coli* was lysed under anaerobiosis with acid-washed glass beads, and DNase1 and MgCl2 (10 mM) were added to the extracts. Experiments under anaerobiosis were performed in a glove box (Jacomex, France) under constant argon flow. Protein concentration was quantified by the Bradford assay (Bio-Rad). $Gpx3^{C82S}$ was purified by the same procedure.

Peroxidase Assays

Peroxidase activity was monitored by the spectrometric determination of NADPH consumption at 340 nm. The reaction was carried out in a buffer containing Tris-Cl [pH 8] (100 mM), NADPH (0.3 mM) (Sigma), and either *E. coli* thioredoxin 1.34 μM (Sigma) and *E. coli* thioredoxin reductase (0.18 μM) (Sigma), or GSH (0.3 to 3 mM) (Sigma) and *S. cerevisiae* glutathione reductase (2 μM) (Sigma). Purified Gpx3 (2.5 μg = 1.35 μM) was added to a 100 μl final reaction volume and the reaction was started 1 min later by adding H_2O_2 (100 μM).

LC-MS/MS and MS/MS analyses

Proteins in gel slices were digested by trypsin or chymotrypsin, as described (Shevchenko et al., 1996). Half of the sample was reduced by DTT and alkylated with iodoacetamide before digestion. For the identification of Gpx3, the tryptic digest of the $Yap1^{303A}$ high MW band was analyzed by nanoscale capillary liquid chromatography-tandem mass spectrometry (LC-MS/MS), using an UltiMate capillary LC system (LC Packings, Amsterdam) connected to an ESI-QqTOF hybrid mass spectrometer (Q-TOF2, Micromass, Manchester, UK). Chromatographic separations were conducted on a reversed-phase (RP) capillary column (Pepmap C18, 75 μm i.d., 15 cm length, LC Packings) at a 200 nL/min flow, with a linear gradient from 100% A (H_2O/acetonitrile/FA, 96/4/0.1, v:v) to 50% B (H_2O/acetonitrile/FA, 10/90/0.085, v:v) in 50 min, followed by a flush at 100% B. LC-MS/MS data were obtained in an automatic mode and converted into a .PKL file using Masslynx software (Micromass), submitted to Mascot (http://www.matrixscience.com/). Proteins were identified by comparison of experimental data to the NCBInr database. For the identification of disulfide bridges, tryptic or chymotryptic peptides were manually analyzed by tandem mass spectrometry (MS/MS) on the Q-TOF2. Ions with masses corresponding to expected disulfide-linked peptides or to their reduced and alkylated counterparts were detected, selected, and fragmented.

RNA Analysis

Total RNA was extracted as described (Lee et al., 1999). cDNAs were synthetized by random hexanucleotide–primed RT from 1 μg of total RNA. On-line quantitative PCR was performed on a Bio-Rad iCycler using the fluorescent CyberGreen method, with 5 pM of *TRX2*, *TRR1*, or ACT1 specific forward and reverse primers, in triplicate reactions according to the supplier recommendations. The *TRX2/ACT1* or *TRR1/ACT1* treshold cycles ratios were calculated using the iCycler iQ RT software (Bio-Rad).

Acknowledgments

We thank S. Desaint and F. Tacnet for gene expression analysis; J. Acker and J.-M. Buhler for protein purification and V. Labas for MS sample digestion; A. Sentenac for continuous support; and A. Desbois, C. Mann, A. Sentenac, B. Biteau, G. Rousselet, F. Tacnet, T. Picaud, and C. Carles for comments. A special thank to C. Creminon for the 9E10 beads. This work was supported by grants from ARC (4202) to M.B.T., fellowships from FRM to A.D. and from CNRS and L'Oreal to D.P. A special thanks to L. Moisan.

Received: April 19, 2002
Revised: August 29, 2002

References

Avery, A.M., and Avery, S.V. (2001). *Saccharomyces cerevisiae* expresses three phospholipid hydroperoxide glutathione peroxidases. J. Biol. Chem. *276*, 33730–33735.

Bjornstedt, M., Xue, J., Huang, W., Akesson, B., and Holmgren, A. (1994). The thioredoxin and glutaredoxin systems are efficient electron donors to human plasma glutathione peroxidase. J. Biol. Chem. *269*, 29382–29384.

Brigelius-Flohe, R. (1999). Tissue-specific functions of individual glutathione peroxidases. Free Radic. Biol. Med. *27*, 951–965.

Carmel-Harel, O., Stearman, R., Gasch, A.P., Botstein, D., Brown, P.O., and Storz, G. (2001). Role of thioredoxin reductase in the Yap1p-dependent response to oxidative stress in *Saccharomyces cerevisiae*. Mol. Microbiol. *39*, 595–605.

Chae, H.Z., Chung, S.J., and Rhee, S.G. (1994). Thioredoxin-dependent peroxide reductase from yeast. J. Biol. Chem. *269*, 27670–27678.

Claiborne, A., Yeh, J.I., Mallett, T.C., Luba, J., Crane, E.J., Charrier, V., and Parsonage, D. (1999). Protein-sulfenic acids: diverse roles for an unlikely player in enzyme catalysis and redox regulation. Biochemistry *38*, 15407–15416.

Coleman, S.T., Epping, E.A., Steggerda, S.M., and Moye-Rowley, W.S. (1999). Yap1p activates gene transcription in an oxidant-specific fashion. Mol. Cell. Biol. *19*, 8302–8313.

Delaunay, A., Isnard, A.D., and Toledano, M.B. (2000). H_2O_2 sensing through oxidation of the Yap1 transcription factor. EMBO J. *19*, 5157–5166.

Ellis, H.R., and Poole, L.B. (1997). Roles for the two cysteine residues of AhpC in catalysis of peroxide reduction by alkyl hydroperoxide reductase from *Salmonella typhimurium*. Biochemistry *36*, 13349–13356.

Gasch, A.P., Spellman, P.T., Kao, C.M., Carmel-Harel, O., Eisen, M.B., Storz, G., Botstein, D., and Brown, P.O. (2000). Genomic expression programs in the response of yeast cells to environmental changes. Mol. Biol. Cell *11*, 4241–4257.

Godeas, C., Tramer, F., Micali, F., Soranzo, M., Sandri, G., and Panfili, E. (1997). Distribution and possible novel role of phospholipid hydroperoxide glutathione peroxidase in rat epididymal spermatozoa. Biol. Reprod. *57*, 1502–1508.

Gonzalez-Flecha, B., and Demple, B. (2000). Genetic responses to free radicals. Homeostasis and gene control. Ann. N Y Acad. Sci. *899*, 69–87.

Inoue, Y., Matsuda, T., Sugiyama, S., Izawa, S., and Kimura, A. (1999). Genetic analysis of glutathione peroxidase in oxidative stress response of *Saccharomyces cerevisiae*. J. Biol. Chem. *274*, 27002–27009.

Izawa, S., Maeda, K., Sugiyama, K., Mano, J., Inoue, Y., and Kimura, A. (1999). Thioredoxin deficiency causes the constitutive activation of Yap1, an AP-1-like transcription factor in *Saccharomyces cerevisiae*. J. Biol. Chem. *274*, 28459–28465.

Kim, S.O., Merchant, K., Nudelman, R., Beyer, W.F., Jr., Keng, T., DeAngelo, J., Hausladen, A., and Stamler, J.S. (2002). OxyR: a molecular code for redox-related signaling. Cell *109*, 383–396.

Kuge, S., and Jones, N. (1994). YAP1 dependent activation fo TRX2 is essential for the response of *Saccharomyces cerevisiae* to oxidative stress by hydroperoxides. EMBO J. *13*, 655–664.

Kuge, S., Jones, N., and Nomoto, A. (1997). Regulation of yAP-1 nuclear localization in response to oxidative stress. EMBO J. *16*, 1710–1720.

Kuge, S., Toda, T., Lizuka, N., and Nomoto, A. (1998). Crm1 (Xpo1) dependent nuclear export of the budding yeast transcription factor yAP-1 is sensitive to oxidative stress. Genes Cells *3*, 521–532.

Kuge, S., Arita, M., Murayama, A., Maeta, K., Izawa, S., Inoue, Y., and Nomoto, A. (2001). Regulation of the yeast Yap1p nuclear export signal is mediated by redox signal-induced reversible disulfide bond formation. Mol. Cell. Biol. *21*, 6139–6150.

Lee, J., Godon, C., Lagniel, G., Spector, D., Garin, J., Labarre, J., and Toledano, M.B. (1999). Yap1 and Skn7 control two specialized oxidative stress response regulons in yeast. J. Biol. Chem. *274*, 16040–16046.

Maiorino, M., Flohe, L., Roveri, A., Steinert, P., Wissing, J.B., and Ursini, F. (1999). Selenium and reproduction. Biofactors *10*, 251–256.

Pomposiello, P.J., and Demple, B. (2001). Redox-operated genetic switches: the SoxR and OxyR transcription factors. Trends Biotechnol. *19*, 109–114.

Shevchenko, A., Wilm, M., Vorm, O., and Mann, M. (1996). Mass spectrometric sequencing of proteins silver-stained polyacrylamide gels. Anal. Chem. *68*, 850–858.

Sikorski, R.S., and Hieter, P. (1989). A system of shuttle vectors and yeast host strains designed for efficient manipulation of DNA in *Saccharomyces cerevisiae*. Genetics *122*, 19–27.

Spector, D., Labarre, J., and Toledano, M.B. (2000). A genetic investigation of the essential role of glutathione: mutations in the proline biosynthesis pathway are the only suppressors of glutathione auxotrophy in yeast. J. Biol. Chem. *276*, 7011–7016.

Ursini, F., Heim, S., Kiess, M., Maiorino, M., Roveri, A., Wissing, J., and Flohe, L. (1999). Dual function of the selenoprotein PHGPx during sperm maturation. Science *285*, 1393–1396.

Ursini, F., Maiorino, M., Brigelius-Flohe, R., Aumann, K.D., Roveri, A., Schomburg, D., and Flohe, L. (1995). Diversity of glutathione peroxidases. Methods Enzymol. *252*, 38–53.

Ursini, F., Maiorino, M., and Roveri, A. (1997). Phospholipid hydroperoxide glutathione peroxidase (PHGPx): more than an antioxidant enzyme? Biomed. Environ. Sci. *10*, 327–332.

Vido, K., Spector, D., Lagniel, G., Lopez, S., Toledano, M.B., and Labarre, J. (2000). A proteome analysis of the cadmium response in *Saccharomyces cerevisiae*. J. Biol. Chem. *276*, 8469–8474.

Wu, A., Wemmie, J.A., Nicholas, P., Edgington, N.P., Goebl, M., Guevara, J.L., and Moye-Rowley, W.S. (1993). Yeast bZip proteins mediate pleiotropic drug and metal resistance. J. Biol. Chem. *268*, 18850–18858.

Yan, C., Lee, L.H., and Davis, L.I. (1998). Crm1p mediates regulated nuclear export of a yeast AP-1-like transcription factor. EMBO J. *17*, 7416–7429.

Zheng, M., Aslund, F., and Storz, G. (1998). Activation of the OxyR transcription factor by reversible disulfide bond formation. Science *279*, 1718–1721.